Activation of Phosphatidylinositol-Specific Phospholipase C by HDL-Associated Lysosphingolipid. Involvement in Mitogenesis but Not in Cholesterol Efflux†

Jerzy-Roch Nofer,*,‡,§ Manfred Fobker,‡ Gunnar Höbbel,§ Reinhard Voss,§ Iza Wolinska,§ Martin Tepel,|| Walter Zidek,|| Ralf Junker,‡ Udo Seedorf,§ Arnold von Eckardstein,‡,§ Gerd Assmann,‡,§ and Michael Walter‡,§

Institut für Klinische Chemie und Laboratoriumsmedizin, Westfälische Wilhelms-Universität, Münster, Germany, Institut für Arteriosklerosеforschung an der Universität Münster, Münster, Germany, and Universitätsklinik Marienhospital der Ruhr-Universität Bochum, Herne, Germany

Received May 23, 2000; Revised Manuscript Received September 12, 2000

ABSTRACT: Our earlier studies demonstrated that high-density lipoproteins (HDLs) stimulate multiple signaling pathways, including activation of phosphatidylcholine-specific phospholipases C and D (PC-PLs) and phosphatidylinositol-specific phospholipase C (PI-PLC). However, only activation of PC-PLs was linked to the HDL-induced cholesterol efflux. In the study presented here, the role of HDL-induced PI-PLC activation was studied. In human skin fibroblasts, HDL potently induced PI-PLC as inferred from enhanced phosphatidylinositol bisphosphate ($PtdInsP_2$) turnover and Ca^{2+} mobilization. The major protein component of HDL, apo A-I, did not induce $PtdInsP_2$ turnover or Ca^{2+} mobilization in these cells. Both HDL and apo A-I promoted cellular cholesterol efflux, whereas only HDL induced fibroblast proliferation. Inhibition of PI-PLC with U73122 or blocking intracellular Ca^{2+} elevation with Ni^{2+} or EGTA markedly reduced the extent of HDL-induced cell proliferation but had no effect on cholesterol efflux. In fibroblasts from patients with Tangier disease which are characterized by defective cholesterol efflux, neither HDL-induced $PtdInsP_2$ breakdown and Ca^{2+} mobilization nor cell proliferation was impaired. HDL-induced fibroblast proliferation, $PtdInsP_2$ turnover, and Ca^{2+} mobilization were fully mimicked by the lipid fraction isolated from HDL. Analysis of this fraction with high-performance liquid chromatography (HPLC) and time-of-flight secondary ion mass spectroscopy (TOF-SIMS) revealed that the PI-PLC-inducing activity is identical with two bioactive lysosphingolipids, namely, lysosulfatide (LSF) and sphingosylphosphorylcholine (SPC). Like native HDL, LSF and SPC induced $PtdInsP_2$ turnover, Ca^{2+} mobilization, and fibroblast proliferation. However, both compounds did not promote cholesterol efflux. In conclusion, two agonist activities are carried by HDL. Apo A-I stimulates phosphatidylcholine breakdown and thereby facilitates cholesterol efflux, whereas LSF and SPC trigger PI-PLC activation and thereby stimulate cell proliferation.

Numerous epidemiological studies revealed an inverse association between HDL cholesterol levels and the risk for coronary artery disease (*1*, *2*). This finding is usually explained by the ability of HDL to remove cholesterol from peripheral cells for delivery to the liver and excretion in the bile, a process termed reverse cholesterol transport (*3*, *4*). In addition, HDL has been shown to act as a potent mitogen in vascular smooth muscle cells (*5*), endothelial cells (*6*), lymphocytes (*7*), and other cell types.

Several studies demonstrated that interaction of HDL with cells induces multiple signaling pathways, including activation of phosphatidylcholine-specific phospholipases C and D (PC-PLC[1] and PC-PLD, respectively) and phosphatidylinositol-specific phospholipase C (PI-PLC) (*8*−*13*). Earlier work from our laboratory showed that only HDL-induced phosphatidylcholine breakdown was affected by cholesterol loading of the cells (*13*). Furthermore, pharmacological inhibition of PC-PLC or PC-PLD decreased the extent of HDL-mediated excretion of intracellular cholesterol, whereas products of phosphatidylcholine breakdown mimicked the ability of HDL to stimulate cholesterol efflux (*11*, *13*). Impaired phosphatidylcholine turnover was noted in fibroblasts with defective cholesterol efflux (Tangier disease) (*13*). Taken together, these observations suggest that phosphatidylcholine-specific phospholipases are involved in the HDL-induced efflux of cellular cholesterol. In contrast, the physiological relevance of the PI-PLC activation by HDL remains unknown. In the study presented here, we demon-

† This work was supported by a grants from Innovative Medizinische Forschung (IMF) Foundation to J.-R.N. and M.W. and from Interdisziplinäres Zentrum für Klinische Forschung (IZKF) to A.v.E.

* To whom correspondence should be addressed: Institut für Klinische Chemie und Laboratoriumsmedizin, Universität Münster, Albert Schweitzer Str. 33, 48-129 Münster, Germany. Fax: ++49-251-8347227. Telephone: ++49-173-2706840. E-mail: nofer@uni-muenster.de.

‡ Institut für Klinische Chemie und Laboratoriumsmetizin Westfälische Wilhelms-Universität, Münster.

§ Institut für Arterioskleroseforschung an der Universität Münster.

|| Universitätsklinik Marienhospital der Ruhr-Universität Bochum.

[1] Abbreviations: BrdU, bromodeoxyuridine; FCS, fetal calf serum; HPLC, high-performance liquid chromatography; LSF, lysosulfatide; PC-PLC, phosphatidylcholine-specific phospholipase C; PC-PLD, phosphatidylcholine-specific phospholipase D; PI-PLC, phosphatidylinositol-specific phospholipase C; PKC, protein kinase C; $PtdInsP_2$, phosphatidylinositol 4,5-bisphosphate; SPC, sphingosylphosphorylcholine.

10.1021/bi001162a CCC: $19.00
Published on Web 11/11/2000

strate that activation of PI-PLC is not involved in the HDL-induced efflux of cellular cholesterol but is required for the mitogenic effects exerted by these lipoproteins.

MATERIALS AND METHODS

Materials. 1-(6-{[17β-3-Methoxyestra-1,3,5(10)-trien-17-yl]amino}hexyl)-1-pyrrole-2,5-dione (U73122) and FURA-2 were purchased from Calbiochem (Bad Soden, Germany). [^{33}P]Orthophosphoric acid was from NEN Du Pont (Dreieich, Germany). All other reagents were of the highest available purity and were obtained from Sigma-Aldrich Chemie GmbH (Deisenhofen, Germany). All solvents were HPLC grade and were purchased from Baker GmbH (Gross-Gerau, Germany).

Preparation of Fibroblasts. Human skin fibroblasts were obtained from five normolipidemic healthy probands and from two homozygous patients with familial analphalipoproteinemia (Tangier disease). The cells were maintained in DMEM containing 10% fetal calf serum (FCS), 2 mM L-glutamine, and a 1% antibiotic/antimycotic solution. At the state of preconfluence, cells were incubated for 48 h at 37 °C in DMEM supplemented with free 0.5 mM mevalonolactone. Preliminary results showed that treatment of cells with mevalonolactone increased the rate of HDL-dependent cholesterol efflux by 40−50%. Furthermore, the precision and accuracy of efflux measurements could markedly be improved when the cells were treated with the water-soluble cholesterol precursor instead of loading with insoluble cholesterol. Fibroblasts were made quiescent by incubation with FCS-free medium for 48 h. All experiments were performed with quiescent fibroblasts.

Lipoprotein and Apolipoprotein Isolation. HDL (d = 1.125−1.210 g/mL) was isolated from human plasma by discontinuous KBr gradients as described by Havel et al. (*14*) and dialyzed against 0.3 mmol/L Tris-HCl and 0.14 mol/L NaCl (pH 7.2). Apolipoprotein A-I (apo A-I) was isolated as described previously (*15*). Contamination with other lipoproteins was excluded by analytical isoelectric focusing.

Cholesterol Mass Efflux Measurement. Cell layers were incubated with various agonists for 2 h at 37 °C in DMEM and HEPES containing 1.0 g/L albumin. After incubation, the cell culture media were collected and the total cholesterol mass therein as well as in cell-free incubations with HDL and other agonists was measured by gas−liquid chromatography as described previously (*16*). This method together with the mevolonolactone treatment protocol allowed for high reproducibility of measurements (*17*). Briefly, the efflux media were collected and centrifuged to remove floating cells. Five micrograms of 5β-cholestan-3α-ol was added as the internal standard. To cleave ester bonds, efflux media were then mixed with equal volumes of a KOH/ethanol mixture (2:3, v/v) and incubated at 80 °C for 1 h. Lipids were extracted twice with 1 volume of hexane. The hydrophobic phases were combined and evaporated under the stream of nitrogen. Derivatization to trimethylsilyl ether was performed thereafter according to standard procedures described by Klansek et al. (*18*). After evaporation of the derivatization reagent, the extract was dissolved in 50 μL of a hexane/pyridine mixture (95:5, v/v). Chromatography was carried out using a Dani 8521a gas chromatograph (Monza, Italy) equipped with a programmable injector (PTV), a CP-Wax 57CB fused silica capillary column (25 m × 0.32 mm i.d., 0.2 μm film thickness, Chromspec, Bridgewater, NJ), a flame ionization detector, and a chromatogram data processor MT2 (Kontron, Neufahrn, Germany). Preliminary results showed that a very short incubation with HDL (ca. 30 s) leads to a decrease in total cholesterol mass in the medium likely due to binding of HDL to cells and/or equilibration of HDL cholesterol with cell membranes. For this reason, the results were corrected for the initial uptake of cholesterol from HDL as well as for cholesterol content in cell-free incubations with HDL.

Assessment of DNA Synthesis. DNA synthesis in fibroblasts was assessed by measuring the extent of bromdeoxyuridine (BrdU) incorporation into DNA with a commercially available ELISA (Roche, Mannheim, Germany). Subconfluent quiescent fibroblasts were incubated with various stimulating agents for 20 h. BrdU (100 μmol/L) was added for the final 3−4 h of incubation. Cells were washed twice with PBS, fixed, and permeabilized according to the manufacturer's instructions. Peroxidase-linked anti-BrdU antibody was then added for 2 h. The absorbance was recorded at 420 nm with the Dynatech MR600 96-well plate reader.

Assessment of Phosphatidylinositol 4,5-Bisphosphate Turnover. Quantitation of the phosphatidylinositol 4,5-bisphosphate ($PtdInsP_2$) turnover was carried out as previously described (*19*, *20*). Briefly, fibroblasts were incubated for 4 h at 37 °C with 100 mCi/L [^{32}P]orthophosphoric acid in phosphate-free DMEM containing 20 mmol/L HEPES, washed with PBS, incubated with PBS containing 1.0 g/L albumin, and stimulated with agonist. At different time points, reactions were terminated by scraping the cells off the dishes with 0.5 mL of ice-cold 0.15 mmol/L NaCl. Cell homogenate was added to 1.5 mL of an ice-cold chloroform/methanol/hydrochloric acid mixture (2:1:0.01, v/v/v). Phases were split by adding 0.5 mL of chloroform and 0.5 mL of water, and lipid phases were collected. Water soluble phases were extracted once more with chloroform. For quantitation of [^{32}P]$PtdInsP_2$ by thin-layer chromatography, potassium oxalate-impregnated silica 60 plates were developed with a chloroform/methanol/acetone/acetic acid/water mixture (60:20:23:18:12, v/v). Bands corresponding to radiolabeled phospholipids were visualized using a Bio-Imager (Fuji Bas-KR 1500, Raytest, Germany) and quantified with a TINA data evaluation processor. Identities of labeled bands were determined on the basis of the R_f of authentic phospholipids.

Determination of the Intracellular Ca^{2+} Concentration. The intracellular Ca^{2+} concentration was measured using Ca^{2+} sensitive fluorescence dye FURA-2 as described previously (*20*, *21*). Fibroblasts grown on round coverslips according to the method of Capponi et al. (*22*) were incubated with 2 μmol/L cell-permeant FURA-2 acetoxy methyl ester for 60 min at 37 °C. After loading, the experiments were continued only when a cell viability of >95% was observed by trypan blue exclusion. After the loading period, coverslips were inserted into a quartz cuvette with 2 mL of PBS containing 1 g/L albumin. The fluorescence intensity was recorded at 37 °C using the RF-5001 PC spectrofluorophotometer (Shimadzu, Tokyo, Japan) with alternate excitation wavelengths of 340 and 380 nm (bandwidth, 5 nm) and an emission wavelength of 510 nm (bandwidth, 5 nm). The intracellular calcium concentration was calculated as previously described. Briefly, the maximum

fluorescence was obtained after addition of 1.0 mM digitonin. The minimum fluorescence was obtained after addition of 5 mM EGTA. The ratio out of the measured fluorescence values was calculated. $[Ca^{2+}]_i$ was obtained according to the equation $[Ca^{2+}]_i = K^*(R - R_{min})/(R_{max} - R)$, where R_{min} stands for the ratio in calcium-free solution, R_{max} for the ratio at calcium saturation, and K^* for $K_d(F_{min2}/F_{max2})$, F_{min2} and F_{max2} representing the fluorescence maximum and minimum at 380 nm excitation, respectively. The K_d of FURA-2 was set to 224 nM.

Extraction and Separation of the HDL Lipid Fraction. Native HDL (0.1 mL, 10 g/L) was diluted with 0.9 mL of water adjusted to pH 3 with sulfuric acid and subsequently mixed with 1.0 mL of acetonitrile. After addition of 0.5 g of NaCl, the sample was vortexed and centrifuged (5 min at 800*g*). The upper organic phase arbitrarily called the HDL lipid fraction was transferred to a glass tube and dried over sodium sulfate. Thereafter, the lipid fraction was dissolved in ethanol and rapidly injected into PBS while vortexing. The final amount of ethanol did not exceed 0.1% (v/v). The suspension containing large multilamellar vesicles was placed on ice and sonicated (3 × 1 min) under a continuous stream of nitrogen. The lower aqueous phase containing apoproteins was arbitrarily called the HDL protein fraction, collected, and lyophilized. The protein fraction was dissolved in PBS. Both fractions were used for cell stimulation in amounts indexed to the original HDL concentration. HPLC analysis of the HDL lipid fraction was performed on a Kontron liquid chromatograph with two model 422 pumps and a model 440 diode array detector. The HDL sample (0.03 mL) was introduced onto a column using a Rheodyne 7125 loop injector (Cotati, CA). The separation was carried out on a 5 μm Nucleosil 100-Si column (25 cm × 4 mm i.d.) (Macherey-Nagel, Düren, Germany) with a flow rate of 1.0 mL/min at an ambient temperature. Mobile phase component A was acetonitrile, and component B was an acetonitrile/water mixture (80:20, v/v). The following gradient was used: 100% A at 0 min, 10% A at 45 min, 10% A at 47 min, and 100% at 48 min (end of run at 55 min). Phospholipids were detected by UV absorption at 193 nm.

Time-of-Flight Secondary Ion Mass Spectroscopy (TOF-SIMS). Mass spectrometry was performed on a TOF-SIMS II instrument (ION-TOF, Münster, Germany) as previously described (*23*, *24*). Briefly, 1.0 μL of HPLC fractions was applied to a silver target (galvanic deposited silver layers on a platinum substrate). After evaporation of the solvent, the resulting submonolayer was analyzed by TOF-SIMS [primary ion current, 10^{11} $^{40}Ar^+$ ions/cm^2 (11 keV); mass resolution $m/\Delta m$ of ≈3000 (m is the peak mass and Δm is the peak widths at half-widths of full maximum); typical acquisition time of 90 s]. Masses are expressed in atomic mass units (amu).

RESULTS

Effect of HDL and Apo A-I on Cholesterol Mass Efflux and DNA Synthesis in Human Fibroblasts. Because of the low capacity of apo A-I to bind free cholesterol, efflux experiments were performed in the presence of albumin (1.0 g/L) as an unspecific cholesterol acceptor. Panels A and B of Figure 1 show time kinetics and dose dependence of cholesterol efflux in the presence of HDL and apo A-I, respectively. During the first 2 h of incubation and at a concentration of <0.1 g/L, HDL and apo A-I were equally effective inducers of cholesterol efflux. At longer incubation times or at higher concentrations, HDL became more effective than apo A-I. The minimal HDL and apo A-I concentration required for cholesterol efflux was 0.005 g/L HDL or apo A-I, whereas saturation was reached at 0.5 g/L HDL or apo A-I.

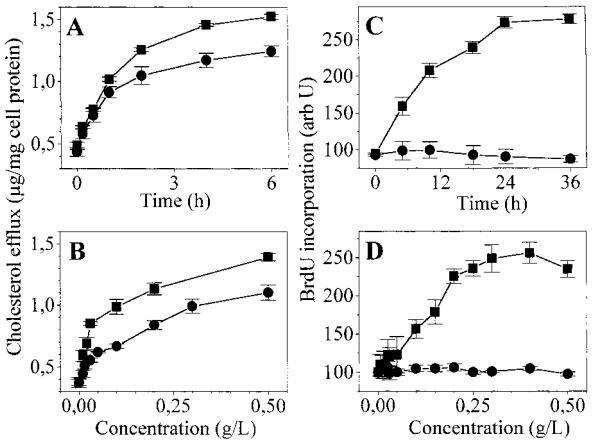

FIGURE 1: Effect of HDL and apo A-I on cholesterol efflux and cell proliferation in human fibroblasts. (A and B) Fibroblasts were incubated with 0.5 g/L HDL (■) or 0.25 g/L apo A-I (●) for the indicated time periods (A) or with increasing concentrations of HDL or apo A-I for 2 h (B). After the indicated periods of time, efflux media were collected and the total cholesterol mass was measured by gas−liquid chromatography as described in Materials and Methods. Data are expressed as means ± the standard deviation from three or four separate determinations. (C and D) Fibroblasts were incubated with 0.5 g/L HDL (■) or 0.25 g/L apo A-I (●) for the indicated periods of time (C) or with increasing concentrations of HDL or apo A-I for 18 h (D). Three hours prior to the end of each incubation, 100 μmol/L BrdU was added. Data are expressed as means ± the standard deviation from six to eight determinations. Control cultures without agonists showed no significant BrdU incorporation.

The stimulatory effects of HDL and apo A-I on cell proliferation in quiescent fibroblasts were investigated by monitoring BrdU incorporation into DNA under strict serum- and growth factor-free conditions. As shown in Figure 1C, HDL (0.5 g/L) induced time-dependent BrdU incorporation, which peaked approximately 24 h after stimulation and remained elevated thereafter. In contrast, BrdU incorporation remained at a control level, when fibroblasts were incubated with apo A-I at a concentration of 0.25 g/L. The extent of BrdU incorporation increased dose-dependently in the presence of 0.1−0.5 g/L HDL (Figure 1D). No effect of apo A-I at a concentration of ≤0.5 g/L on BrdU incorporation was noted.

Effect of HDL and Apo A-I on [^{33}P]PtdInsP$_2$ Turnover in Human Fibroblasts. PI-PLC activation was assessed by monitoring the HDL- and apo A-I-induced breakdown of PtdInsP$_2$ in [^{32}P]orthophosphoric acid-labeled fibroblasts. As shown in Figure 2, addition of 0.5 g/L HDL to fibroblasts produced a rapid decrease in the level of endogenous PtdInsP$_2$. The level of ^{32}P-labeled PtdInsP$_2$ fell to 38% of the initial value within 30 s of stimulation. Thereafter, PtdInsP$_2$ levels rose and normalized after 120 s. To confirm the involvement of PI-PLC in the HDL-induced PtdInsP$_2$

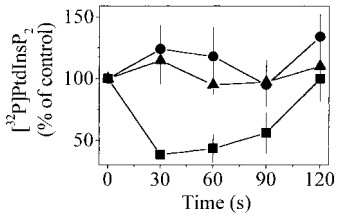

FIGURE 2: Time course of [^{32}P]PtdInsP_2 turnover in human fibroblasts exposed to HDL or apo A-I. ^{32}P-labeled fibroblasts were incubated for the indicated periods of time with with 0.5 g/L HDL (■) or 0.25 g/L apo A-I (●). In some experiments, cells were preincubated for 30 min with 10 μmol/L U73122 (▲). Inositol phospholipids were extracted and separated by thin-layer chromatography as described in Materials and Methods. Changes in the amount of ^{32}P radioactivity are expressed as a percentage of controls representing the amount of radioactivity of [^{32}P]PtdInsP in not stimulated fibroblasts. The phospholipid radioactivity in unstimulated fibroblasts did not change over the time course of the experiments. The data are expressed as means ± the range from two separate determinations.

turnover, the experiments were performed in the presence of U73122, a selective PI-PLC inhibitor. As shown in Figure 2, pretreatment of fibroblasts for 30 min with U73122 (10 μmol/L) prior to the addition of 0.5 g/L HDL completely inhibited PtdInsP_2 breakdown. In contrast to HDL, apo A-I (0.25 g/L) failed to cause a depletion in the level of [^{32}P]-PtdInsP_2 during a 2 min time course (Figure 2).

Effect of HDL and Apo A-I on the Intracellular Ca^{2+} Concentration ($[Ca^{2+}]_i$) in Human Fibroblasts. The PI-PLC-mediated PtdInsP_2 breakdown leads to the liberation of inositol 1,4,5-trisphosphate, which releases Ca^{2+} from intracellular stores and triggers extracellular Ca^{2+} entry. To further examine the effect of HDL and apo A-I on the PI-PLC-induced signal transduction, changes of the free intracellular Ca^{2+} concentration ($[Ca^{2+}]_i$) were determined using the calcium-sensitive fluorescent dye FURA-2. The resting $[Ca^{2+}]_i$ level in fibroblasts averaged 131 ± 43 nmol/L (n = 27). As illustrated in Figure 3A, addition of 0.5 g/L HDL resulted in a time-dependent increase in the intracellular level of calcium. Within 50 s, $[Ca^{2+}]_i$ rose by 166 ± 41 nmol/L (n = 8) over the resting level. $[Ca^{2+}]_i$ decreased thereafter, but remained elevated over the basal level for at least 5 min. The HDL-induced Ca^{2+} release was concentration-dependent (Figure 3B). $[Ca^{2+}]_i$ elevation was observed at a threshold HDL concentration between 0.05 and 0.1 g/L, whereas maximal effects were seen after stimulation with 0.5 g/L HDL. Apo A-I at concentrations 0.01, 0.05, 0.10, and 0.25 g/L failed to stimulate elevation of the intracellular Ca^{2+} level (Figure 3A,B). To examine the involvement of PI-PLC in HDL-induced Ca^{2+} liberation, the effect of U73122 on the elevation of HDL-triggered $[Ca^{2+}]_i$ was tested. In the presence of 10 μM U73122, the HDL-induced $[Ca^{2+}]_i$ increase was markedly inhibited and averaged 9 ± 2 nmol/l (n=3) over the resting level (Figure 3A). To test whether HDL-stimulated intracellular calcium elevation occurs as a consequence of increased Ca^{2+} entry, the experiments were also performed in the presence of Ni^{2+} which blocks divalent cation entry pathways, or in the absence of extracellular Ca^{2+}. As shown in Figure 3C, addition of 5 mM Ni^{2+} markedly reduced the HDL-induced increase in the Ca^{2+} concentration, which was elevated by 41 ± 12 nmol/L (n = 6) over the resting level. A similar effect was observed after chelating extracellular Ca^{2+} with EGTA (1.0 mmol/L). Under this

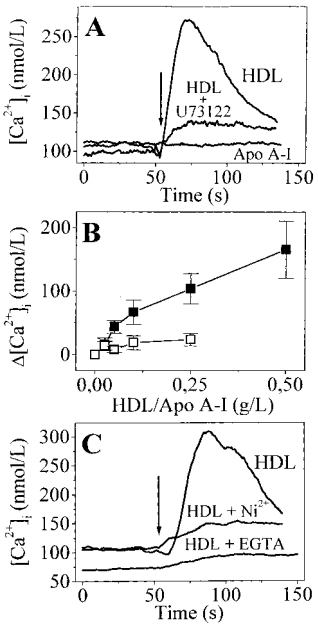

FIGURE 3: Effect of HDL and apo A-I on the Ca^{2+} concentration increase in human fibroblasts. Fibroblasts were loaded with the calcium-sensitive dye FURA-2-AM. In some experiments, cells were preincubated for 30 min with 10 μmol/L U73122 and 5 mmol/L Ni^{2+} or placed in a Ca^{2+}-free solution containing 1 mmol/L EGTA. Cells were then exposed to 0.5 g/L HDL or 0.25 g/L apo A-I, and the fluorescence was recorded as described in Materials and Methods. (A and C) Original tracings obtained from one representative experiment were superimposed for comparison. (B) Line graph showing intracellular calcium concentration increases ($[Ca^{2+}]_i$) induced by various HDL (■) or apo A-I (□) concentrations. Data represent means ± the standard deviation from at least nine separate determinations.

experimental condition, addition of 0.5 g/L HDL raised $[Ca^{2+}]_i$ by 31 ± 8 nmol/L (n = 4) over the resting level.

Effect of PI-PLC and Ca^{2+} Entry Inhibition on HDL-Induced Cholesterol Efflux and Fibroblast Proliferation. The role of PI-PLC in the HDL-induced cholesterol efflux and cell proliferation was approached by testing effects of U73122, Ni^{2+}, and EGTA on both physiological responses. As demonstrated in Figure 4A, pretreatment of fibroblasts for 30 min with 10 μmol/L U73122 prior to the addition of 0.5 g/L HDL inhibited BrdU incorporation into DNA in a concentration-dependent fashion. In contrast, the level of HDL-induced cholesterol efflux was unchanged or slightly increased under identical experimental conditions. Likewise, inhibition of Ca^{2+} entry with 5 mM Ni^{2+} or 1 mM EGTA severely impaired BrdU incorporation into DNA evoked by 0.5 g/L HDL (Figure 4B,C), but did not affect HDL-induced cholesterol efflux.

Effect of HDL on Cholesterol Mass Efflux, DNA Synthesis, [^{33}P]PtdInsP_2 Turnover, and $[Ca^{2+}]_i$ in Tangier Fibroblasts. The involvement of PI-PLC in the HDL-induced cholesterol efflux and cell proliferation was further investigated in Tangier fibroblasts, since these cells are characterized by a defective cholesterol efflux in response to HDL and apo A-I. As illustrated in Figure 5A, the ability of HDL to promote net cholesterol mass efflux from Tangier fibroblasts was inhibited. In contrast, HDL exerted similar mitogenic effects on both Tangier and normal fibroblasts (Figure 5B). As shown in Figure 5C, addition of 0.5 g/L HDL produced a rapid decrease in the level of endogenous PtdInsP_2 in both

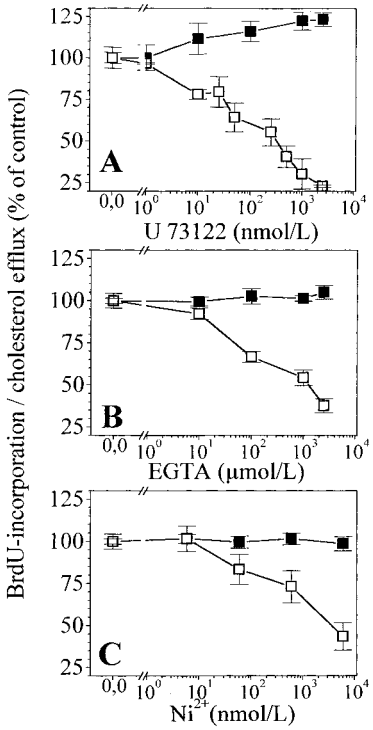

FIGURE 4: Effect of PI-PLC inhibition or Ca^{2+} entry blocking on the HDL-induced cholesterol efflux or cell proliferation in human fibroblasts. Fibroblasts were preincubated for 30 min with 10 μmol/L U73122 (A) or 5 mmol/L Ni^{2+} (B) or placed in a Ca^{2+}-free solution containing 1 mmol/L EGTA (C). Cells were then exposed to 0.5 g/L HDL in a continuous presence of inhibitors, and the levels of cholesterol efflux (■) or BrdU incorporation (□) were measured as described in Materials and Methods. Results are presented as percentages of control values recorded without inhibitors and represent means ± the standard deviation from three (cholesterol efflux) or six to eight (proliferation) separate determinations.

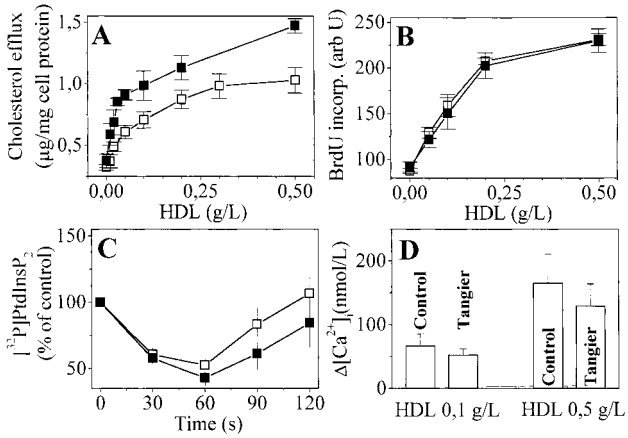

FIGURE 5: Effect of HDL on [^{32}P]$PtdInsP_2$ turnover, Ca^{2+} increase, cholesterol efflux, and cell proliferation in control and Tangier fibroblasts. Normal (■) and Tangier (□) fibroblasts were exposed to 0.5 g/L HDL for various periods of time or to various HDL concentrations. [^{32}P]$PtdInsP_2$ turnover (A), Ca^{2+} increase (B), cholesterol efflux (C), and cell proliferation (D) were asesses as described in Materials and Methods. Data represent means ± the standard deviation from three (cholesterol efflux) or six to eight (proliferation) separate determinations. In graph A, data represent means ± the range from two separate determinations. The phospholipid radioactivity in unstimulated fibroblasts did not change over the time course of experiments.

Tangier and control fibroblasts. Within 60 s of stimulation, the level of ^{32}P-labeled $PtdInsP_2$ fell to 60 and 52% of the initial value in Tangier and control cells, respectively. Likewise, HDL-triggered $[Ca^{2+}]_i$ elevation did not differ among both cell types (Figure 5D). Addition of 0.1 g/L HDL produced an increase in the intracellular level of calcium by 53 ± 9 nmol/L (n = 6) and by 67 ± 19 nmol/L (n = 6) over the resting level in Tangier and normal fibroblasts, respectively. In the presence of 0.5 g/L HDL, $[Ca^{2+}]_i$ rose by 130 ± 34 nmol/L (n = 6) and by 166 ± 45 nmol/L (n = 5) over the resting level in Tangier and normal fibroblasts, respectively.

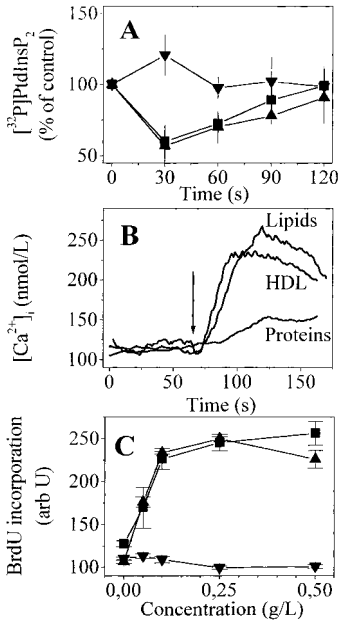

FIGURE 6: Effect of HDL lipid and protein fractions on [^{32}P]-$PtdInsP_2$ turnover, Ca^{2+} concentration increase, and cell proliferation in human fibroblasts. Fibroblasts were exposed to 0.5 g/L HDL (■), HDL lipid fraction (▲), or HDL protein fraction (▼) at concentrations equivalent to 0.5 g/L HDL. (A) After indicated periods of time, the level of [^{32}P]$PtdInsP_2$ was determined as described in Materials and Methods. The phospholipid radioactivity in unstimulated fibroblasts did not change over the time course of the experiments. The data are expressed as means ± the range from two separate determinations. (B) FURA-2 fluorescence was recorded as described in Materials and Methods. Original tracings obtained from one representative experiment were superimposed for comparison. (C) BrdU incorporation was assessed as described in Materials and Methods. Data are expressed as means ± the standard deviation from six to eight determinations. Control cultures without agonists showed no significant BrdU incorporation.

Effect of HDL Lipid and Protein Fractions on [^{33}P]-$PtdInsP_2$ Turnover, $[Ca^{2+}]_i$, and DNA Synthesis in Human Fibroblasts. We next aimed to determine entities in HDL, which induce PI-PLC activation. First, we studied the effect of HDL lipid and protein fractions on $PtdInsP_2$ breakdown and Ca^{2+} mobilization in human fibroblasts. Addition of the HDL lipid fraction at a concentration equivalent to 0.5 g/L native HDL led to a decrease in the level of endogenous $PtdInsP_2$ to 57% of the initial value within 30 s of stimulation (Figure 6A). Similarly, the HDL lipid fraction raised the intracellular Ca^{2+} level by 139 ± 21 nmol/L (n = 8) over the resting level. In contrast, neither $PtdInsP_2$ turnover nor significant intracellular Ca^{2+} mobilization was observed in fibroblasts stimulated with the HDL protein fraction equivalent to 0.5 g/L native HDL. Finally, we examined the mitogenic effect of HDL lipid and protein fractions. As shown in Figure 6C, the HDL lipid fraction induced BrdU

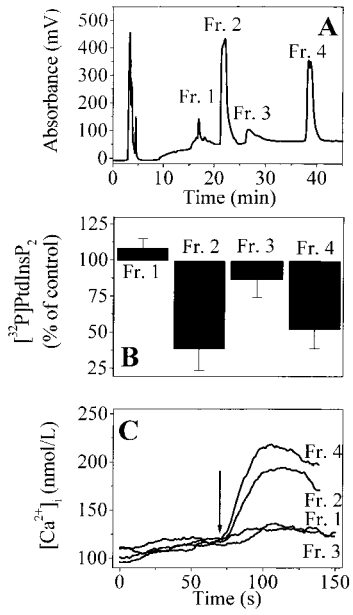

FIGURE 7: Effect of HPLC fractions isolated from HDL lipid fraction on $[^{32}P]PtdInsP_2$ turnover and Ca^{2+} concentration increase in human fibroblasts. (A) HDL lipid fraction isolated from 1.0 g/L HDL was subjected to HPLC on a Nucleosil 100-Si column as described in Materials and Methods. Fractions (Fr.) numbered from 1 to 4 were collected and used for the assessment of $[^{32}P]PtdInsP_2$ turnover and $[Ca^{2+}]_i$ mobilization. A representative chromatogram is shown. (B) Isolated fractions were added to fibroblasts for the indicated periods of time, and the level of $[^{32}P]PtdInsP_2$ was determined as described in Materials and Methods. The amount of phospholipid radioactivity in unstimulated fibroblasts did not change over the time course of the experiments. The data are expressed as means ± the standard deviation from three separate determinations. (C) Ca^{2+} mobilization was monitored in FURA-2-loaded fibroblasts as described in Materials and Methods. Original tracings obtained from one representative experiment were superimposed for comparison.

incorporation into DNA in a concentration-dependent fashion. The maximal effect was observed at a concentration equivalent to 0.25−0.5 g/L native HDL. No effect of the HDL protein fraction on the rate of BrdU incorporation was noted.

Effect of HPLC Lipid Fractions on $[^{33}P]PtdInsP_2$ Turnover and $[Ca^{2+}]_i$ in Human Fibroblasts. To identify the lipid moiety in HDL activating PI-PLC, the HDL lipid fraction was analyzed by HPLC (Figure 7A). HPLC profiles of lipids recorded at 193 nm revealed four distinct fractions which were subsequently tested for their ability to induce $PtdInsP_2$ breakdown and intracellular Ca^{2+} mobilization in human fibroblasts. Fractions were added to fibroblasts at concentrations corresponding to 1.0 g/L HDL. Fractions 2 and 4 contained a signaling activity which induced a depletion of the level of $[^{32}P]PtdInsP_2$ to 52 and 39% of the initial value over a 30 s time course, respectively (Figure 7B). Furthermore, fractions 2 and 4 elevated intracellular Ca^{2+} concentrations by 92 ± 13 nmol/L ($n = 4$) and by 106 ± 16 nmol/L ($n = 8$) over the resting level, respectively (Figure 7C). In contrast, no $PtdInsP_2$ breakdown or Ca^{2+} mobilization was observed after stimulating cells with fractions 1 and 3.

Mass Spectroscopy Analysis of the HPLC Lipid Fractions. Fractions 2 and 4 were subsequently analyzed using time-of-flight secondary ion mass spectroscopy (TOF-SIMS). In the negative and positive secondary ion mass spectra, lipid species were detectable in deprotonated $[M - 2H]^-$, protonated $[M + H]^+$, or intact $[M]^-$ forms. Panels A and B of Figure 8 show spectra in the mass range of the molecular ions, which represented the most intense peaks in the positive and negative spectra. The theoretical masses of the molecular ions for fraction 2 were as follows: $[M]^-$, 542.3 amu; $[M - 2H]^-$, 540.3 amu; for fraction 4, $[M + H]^+ = 465.6$ amu. In addition, a second peak with a molecular mass of 299.5 amu ($[M]^+$) identical with sphingosine was noted in fraction 2 and 4, and a third one with a molecular mass of 184 amu ($[M]^+$) identical with phosphocholine was seen in fraction 4 only (not shown). No peaks typical for polyunsaturated fatty acids were seen in the negative spectra of both fractions. The molecular masses, the presence of sphingosine and phosphocholine, and the absence of fatty acids in the negative spectra of the compounds present in fractions 2 and 4 suggested that the searched bioactive lysosphingolipids correspond to lysosulfatide (LSF) and sphingosylphosphorylcholine (SPC), respectively. The identity of both compounds was confirmed by comparison with mass spectra (Figure 8C,D) and HPLC retention times (Figure 9A,B) of purified LSF and SPC standards. On the basis of the HPLC results for lipid fractions obtained from three separate HDL preparations, the concentrations of LSF and SPC in HDL were estimated to be 6.1 ± 1.2 μmol/mg of protein ($n = 3$) and 4.1 ± 3.4 μmol/mg of protein ($n = 3$), respectively. We also tested for the presence of other biologically active lysosphingolipids in the HDL lipid fraction. On the basis of the HPLC retention times of purified standards, the presence of the following lysosphingolipids in fractions containing signaling activities could be excluded: sphingosine 1-phosphate, psychosine, and glucopsychosine.

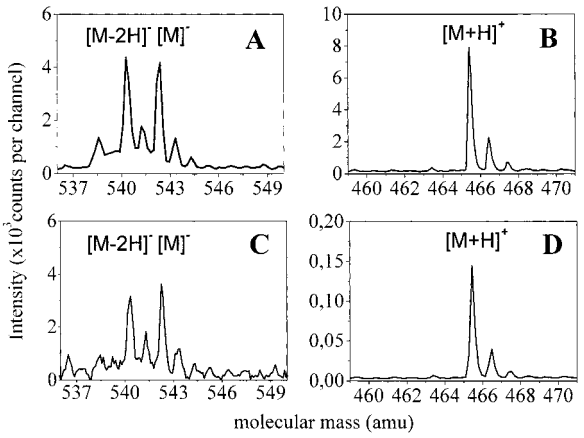

FIGURE 8: Time-of-flight secondary ion mass spectroscopy of HPLC fractions isolated from HDL lipid fraction. HPLC fractions 2 and 4 isolated from HDL lipids were subjected to TOF-SIMS as described in Materials and Methods. The secondary ion mass spectrogram in the mass range of the molecular ions that represented the most intense peaks in fractions 2 (A) and 4 (B) is shown. Mass spectrometry of LSF (C) and SPC (D) standards produced a pattern of fragments identical to those of the HPLC fractions.

Effect of SPC and LSF on Cholesterol Mass Efflux, DNA Synthesis, $[^{33}P]PtdInsP_2$ Turnover, and $[Ca^{2+}]_i$ in Human Fibroblasts. Finally, we tested whether LSF and SPC exert signaling and mitogenic effects similar to those of HDL. As shown in Figure 10A, addition of 10 μmol/L LSF or 10 μmol/L SPC to fibroblasts led to the marked depletion in the level of endogenous $PtdInsP_2$. The level of ^{32}P-labeled $PtdInsP_2$ fell to 52 and 63% of the initial value 30 s after stimulation, respectively. In parallel, LSF and SPC raised

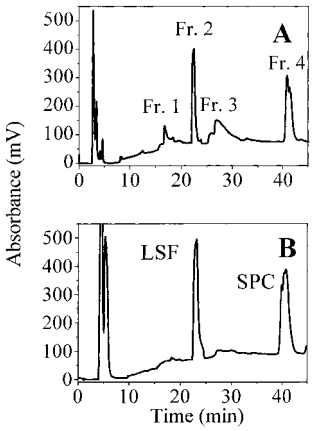

FIGURE 9: HPLC separation of HDL lipid fraction and original LSF and SPC standards. HDL lipid fraction isolated from 1.0 g/L HDL (A) and original LSF and SPC standards (B) were subjected to HPLC on a Nucleosil 100-Si column as described in Materials and Methods. Shown are representative chromatograms.

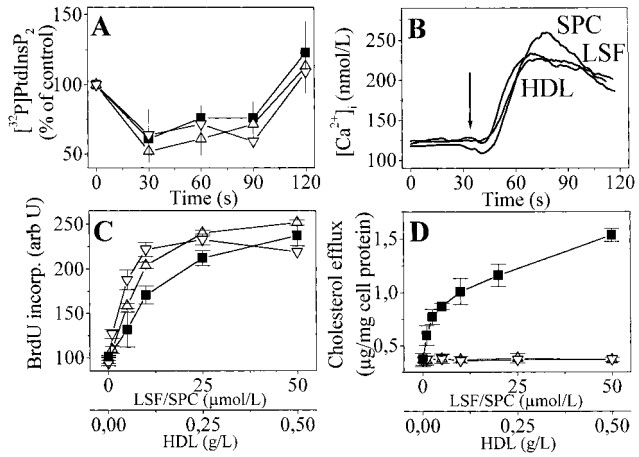

FIGURE 10: Effect of LSF and SPC on [^{32}P]PtdInsP_2 turnover, Ca^{2+} concentration increase, cholesterol efflux, and cell proliferation in control and Tangier fibroblasts. Fibroblasts were exposed to 0.5 g/L HDL (■), 10 μmol/L LSF (▼), or 10 μmol/L SPC (▲) for various periods of time or at various concentrations of HDL, LSF, or SPC. [^{32}P]PtdInsP_2 turnover (A), Ca^{2+} concentration increase (B), cholesterol efflux (C), and cell proliferation (D) were assessed as described in Materials and Methods. Data represent means ± the standard deviation from three (cholesterol efflux) or six to eight (proliferation) separate determinations. In graph A, the data represent means ± the range from two separate determinations. The amount of phospholipid radioactivity in unstimulated fibroblasts did not change over the time course of the experiments.

the intracellular Ca^{2+} concentration by 135 ± 51 nmol/L (n = 7) and 144 ± 40 nmol/L (n = 6) over the resting level, respectively (Figure 10B). Figure 10C demonstrates that both LSF and SPC stimulated BrdU incorporation into DNA in a concentration-dependent fashion. Maximal stimulation was observed at a concentration of approximately 10 μmol/L for both compounds. In contrast, neither LSF nor SPC could mimic the effect of HDL on cholesterol excretion from fibroblasts (Figure 10D).

DISCUSSION

Phosphoinositide-specific phospholipase C (PI-PLC) is a ubiquitously expressed enzyme involved in signaling from numerous agonists (*25*). Previously, formation of several products arising from the phospholipase C-catalyzed cleavage of the phosphatidylinositol 4,5-bisphosphate was observed after stimulation with HDL (*10*−*12*). In addition, several cellular responses associated with PI-PLC activation such as Ca^{2+} mobilization and pH elevation were noted in the presence of HDL (*10*−*12*, *26*−*29*). However, it is not known which of the physiological effects exerted by HDL is mediated the PI-PLC activation. In this report, we demonstrate that PI-PLC activation is required for the strong mitogenic effect of HDL but not for the HDL-induced efflux of cellular cholesterol.

In contrast to cholesterol efflux which was induced by both HDL and apo A-I, cell proliferation, PI-PLC activation, and mobilization of intracellular Ca^{2+} were induced solely by native HDL. Furthermore, the stimulatory effects of HDL on fibroblast proliferation and cholesterol efflux were observed in different agonist concentration ranges. Whereas very low HDL concentrations (0.005−0.01 g/L) were sufficient to induce efflux of cellular cholesterol, the fibroblast proliferation and PI-PLC stimulation were seen at HDL concentrations of ≥0.05 g/L. In another set of experiments, we could demonstrate that the two cellular effects of HDL could be separated by the use of pharmacological inhibitors. U73122, a potent and selective PI-PLC inhibitor, enhanced rather than inhibited HDL-induced cholesterol efflux. Moreover, the HDL-induced cholesterol efflux remained unaffected after blocking Ca^{2+} entry and subsequent $[Ca^{2+}]_i$ elevation with divalent cations (Ni^{2+}) or by chelating extracellular Ca^{2+} with EGTA. In contrast, inhibition of PI-PLC activation with U73122 or blockade of extracellular Ca^{2+} entry reduced the mitogenic effect of HDL. These observations are in agreement with the results of Favre et al. showing a Ca^{2+}-dependent step in the HDL-induced mitogenesis (*30*). Additional evidence supporting the contention that PI-PLC activation is not involved in the regulation of the HDL-mediated cholesterol efflux comes from experiments with Tangier fibroblasts. These cells are characterized by the impaired intracellular cholesterol transport and efflux due to the defect in ABC1 (*31*−*36*). Previously, impaired PI-PLC activation was seen in fibroblasts from Tangier patients after stimulation with HDL (*11*). However, we observed normal proliferation, PtdInsP_2 turnover, and Ca^{2+} mobilization in Tangier fibroblasts in response to HDL, whereas the level of cholesterol efflux was reduced. Thus, abnormal PI-PLC activation cannot account for defective cholesterol translocation and efflux seen in these cells.

Overall, our data document that PI-PLC activation is essential for the HDL-induced cell proliferation. In this respect, HDL resembles several hormones and growth factors such as insulin, FGF, and EGF. Like these compounds, HDL initiates a variety of intracellular signals, some of which appear to be activated by apo A-I and related to cholesterol translocation and efflux. Recently, Garver et al. and Deeg et al. found that distinct sets of proteins underwent phosphorylation in fibroblasts stimulated with HDL or with purified apoproteins (*37*, *38*). In addition, HDL-induced protein phosphorylation was not affected by trypsinization or by covalent modification of HDL apoproteins, suggesting that the lipid moiety can partially account for HDL signaling. This report extends these results by showing that neither apo A-I nor the total protein fraction isolated from HDL was able to activate PI-PLC and to stimulate proliferation in human fibroblasts. On the other hand, PtdInsP_2 breakdown,

Ca^{2+} mobilization, and mitogenesis were induced by a lipid fraction isolated from HDL, indicating the involvement of a lipophilic agonist distinct from apoproteins. With several lines of evidence, this study documents that this agonist is identical with LSF and SPC. First, the mass spectra of the signaling activities found in fractions 2 and 4 were indistinguishable from those of purified LSF and SPC, respectively. Second, the HPLC retention times and peak morphologies of fraction 2 and 4 and those of LSF and SPC were identical. Third, both LSF and SPC mimicked HDL-induced $PtdInsP_2$ breakdown, Ca^{2+} mobilization, and fibroblast proliferation. By contrast, neither of the two compounds induced cholesterol efflux. Fourth, LSF and SPC concentrations found in HDL were sufficiently high to account for cellular effects of these lipoproteins. By HPLC analysis, we failed to detect other biologically active lysosphingolipids such as sphingosine 1-phosphate, psychosine, and glucopsychosine in HDL. The presence of glycerolipids such as lysophosphatidic acid or lysophosphatidylcholine in HDL was excluded by others (*27*, *39*). However, our results do not entirely exclude the possibility that other mitogenic compounds such as sterol derivatives are carried in HDL particles and were lost during extraction and fractionation.

The intracellular signaling events initiated by SPC were extensively studied over recent years (*40*, *41*). Several features of SPC signaling are close to those seen in HDL. In addition to PI-PLC activation and Ca^{2+} mobilization, both agonists were reported to activate mitogen-activated protein kinase ($p42/44^{MAPK1/2}$) and protein kinase C (PKC) (*37*, *38*, *42*−*45*). Both HDL- and SPC-induced MAPK activation are linked to a G_i protein and sensitive to *Pertussis* toxin (*38*, *44*). Furthermore, SPC was demonstrated to act as a potent mitogen in various cell lines, including fibroblasts (*43*, *46*). Like SPC, LSF was found to activate PI-PLC and to increase the intracellular Ca^{2+} concentration in a *Pertussis* toxin- and U73122-dependent manner (*47*). Due to structural similarity, both compounds are thought to act via same receptors, which have recently been identified (*48*).

Bioactive lysosphingolipids evoke a remarkable diversity of cellular responses ranging from stimulation of cell survival and protection from apoptosis to inhibition of cell migration and motility, and stimulation of wound healing (*40*, *41*). Due to their lipophilicity, it was generally assumed that these compounds act in an autocrine or paracrine fashion. By demonstrating that HDLs serve as carriers for LSF and SPC, this study suggests that a much wider spectrum of biological targets may be accessible to lysosphingolipids. Our findings raise the possibility that lysoshingolipids in HDL account for some anti-inflammatory effects exerted by these lipoproteins. Further work is necessary to determine whether these lipids contribute to the antiatherogenic potential of HDL.

REFERENCES

1. Gordon, T., and Rifkind, B. M. (1989) *N. Engl. J. Med. 321*, 1311−1315.
2. Assmann, G., and Schulte, H. (1992) *Am. J. Cardiol. 70*, 733−772.
3. Oram, J. F., and Yokoyama, S J. (1996) *J. Lipid Res. 37*, 2473−2491.
4. Tall, A. (1998) *Eur. Heart J. 19* (Suppl. A), A31−A35.
5. Björkerud, S., and Björkerud, B. (1994) *Arterioscler., Thromb., Vasc. Biol. 14*, 288−298.
6. Chen, J. K., Hoshi, H., McClure, D. B., and McKeehan, W. L. (1986) *J. Cell. Physiol. 129*, 207−214.
7. Favre, G., Blancy, E., Tournier, J. F., and Soula, G. (1989) *Biochim. Biophys. Acta 1013*, 118−124.
8. Walter, M., Reinecke, H., Nofer, J.-R., Seedorf, U., and Assmann, G. (1995) *Arterioscler., Thromb., Vasc. Biol. 15*, 1975−1986.
9. Nofer, J.-R., Walter, M., Kehrel, B., Seedorf, U., and Assmann, G. (1995) *Biochem. Biophys. Res. Commun. 207*, 148−154.
10. Mollers, C., Drobnik, W., Resink, T., and Schmitz, G. (1995) *Cell. Signalling 7*, 695−707.
11. Drobnik, W., Mollers, C., Resink, T., and Schmitz, G. (1995) *Arterioscl., Thromb., Vasc. Biol. 15*, 1369−1377.
12. Bochkov, V., Tkachuk, V., Buhler, F., and Resink, T. (1992) *Biochem. Biophys. Res. Commun. 188*, 1295−1304.
13. Walter, M., Reinecke, H., Gerdes, U., Nofer, J.-R., Höbbel, G., Seedorf, U., and Assmann, G. (1996) *J. Clin. Invest. 98*, 2315−2323.
14. Havel, R. J., Eder, H., and Bragdon, J. H. (1955) *J. Clin. Invest. 3*, 1345−1353.
15. von Eckardstein, A., Funke, H., Walter, M., Altland, K., Benninghoven, A., and Assmann, G. (1990) *J. Biol. Chem. 265*, 8610−8617.
16. Cullen, P., Tegelkamp, K., Fobker, M., Kannenberg, F., and Assmann, G. (1997) *Anal. Biochem. 251*, 39−44.
17. Gambert, P., Lallemant, C., Archambault, A., Maume, B. F., and Padieu, P. (1979) *J. Chromatogr. 162*, 1−6.
18. Klansek, J. J., Yancey, P., St. Clair, R. W., Fisher, R. T., Johnson, W. J., and Glick, J. M. (1995) *J. Lipid Res. 36*, 2261−2266.
19. Nofer, J.-R., Tepel, M., Walter, M., Seedorf, U., Zidek, W., and Assmann, G. (1997) *Circulation 95*, 1370−1377.
20. Nofer, J.-R., Tepel, M., Walter, M., Seedorf, U., Assmann, G., and Zidek, W. (1997) *J. Biol. Chem. 272*, 32861−32868.
21. Tepel, M., Kühnapfel, S., Theilmeier, G., Teupe, C., Schlotman, R., and Zidek, W. (1994) *J. Biol. Chem. 269*, 26239−26242.
22. Capponi, A. M., Lew, P. D., and Vallotton, M. B. (1985) *J. Biol. Chem. 260*, 7836−7842.
23. Seedorf, U., Fobker, M., Voss, R., Meyer, K., Kannenberg, F., Meschede, D., Ullrich, K., Horst, J., Benninghoven, A., and Assmann, G. (1995) *Clin. Chem. 41*, 548−552.
24. Meyer, K., Fobker, M., Christians, U., Erren, M., Sewing, K.-F., Assmann, G., and Benninghoven, A. (1996) *Drug Metab. Dispos. 24*, 151−1154.
25. Williams, R. L. (1999) *Biochim. Biophys. Acta 1441*, 255−267.
26. Bochkov, V. N., Tkachuk, V. A., Hahn, A. W., Bernhardt, J., Buhler, F. R., and Resink, T. J. (1993) *Arterioscler. Thromb. 13*, 1261−1269.
27. Pörn, M. I., Ackermann, K. E. O., and Slotte, J. P. (1991) *Biochem. J. 279*, 29−33.
28. Honda, H. M., Wakamatsu, B. K., Goldhaber, J. I., Berliner, J. A., Navab, M., and Weiss, J. N. (1999) *Atherosclerosis 143*, 299−306.
29. Sachinidis, A., Ko, Y., Wieczorek, A., Weisser, B., Locher, R., Vetter, W., and Vetter, H. (1993) *Biochem. Biophys. Res. Commun. 192*, 794−799.
30. Tazi, K. A., Bonnafous, M., Favre, G., Soula, G., and Le Gaillard, F. (1995) *Biochem. J. 307*, 557−561.
31. Walter, M., Gerdes, U., Seedorf, U., and Assmann, G. (1994) *Biochem. Biophys. Res. Commun. 205*, 850−856.
32. Rogler, G., Trumbach, B., Klima, B., Lackner, K. J., and Schmitz, G. (1995) *Arterioscler., Thromb., Vasc. Biol. 15*, 683−690.
33. Remaley, A. T., Schumacher, U. K., Stonik, J. A., Farsi, B. D., Nazih, H., and Brewer, H. B., Jr. (1997) *Arterioscler., Thromb., Vasc. Biol. 17*, 1813−1821.
34. Brooks-Wilson, A., Marcil, M., Clee, S. M., Zhang, L. H., Roomp, K., van Dam, M., Yu, L., Brewer, C., Collins, J. A., Molhuizen, H. O., Loubser, O., Oulette, B. F., Fichter, K., Ashbourne-Excoffon, K. J., Sensen, C. W., Scherer, S., Mott,

S., Denis, M., Martindale, D., Frohlich, J., Morgan, K., Koop, B., Pimoste, S., Kastelein, J. J., and Hayden, M. R. (1999) *Nat. Genet. 22*, 336−345.
35. Bodzioch, M., Orso, E., Klucken, J., Langmann, T., Bottcher, A., Diedrich, W., Drobnik, W., Barlage, S., Buchler, C., Porsch-Ozcurumez, M., Kaminski, W. E., Hahmann, H. W., Oette, K., Rothe, G., Aslanidis, C., Lackner, K. J., and Schmitz, G. (1999) *Nat. Genet. 22*, 347−351.
36. Rust, S., Rosier, M., Funke, H., Real, J., Amoura, Z., Piette, J. C., Deleuze, J. F., Brewer, H. B., Jr., Duverger, N., Denefle, P., and Assmann, G. (1999) *Nat. Genet. 24*, 352−355.
37. Deeg, M. A., Bowen, R. F., Oram, J. F., and Bierman, E. D. (1997) *Arterioscler., Thromb., Vasc. Biol. 17*, 1667−1674.
38. Garver, W. S., Deeg, M. A., Bowen, R. F., Culala, M. M., Bierman, E. L., and Oram, J. F. (1997) *Arterioscler., Thromb., Vasc. Biol. 17*, 2698−2706.
39. Yuan, Y., Jackson, S. P., Newnham, H. H., Mitchell, C. A., and Salem, H. H. (1995) *Blood 86*, 4166−4174.
40. Moolenaar, W. H. (1999) *Exp. Cell. Res. 253*, 230−238.
41. Hla, T., Menq-Jer, L., Ancellin, N., Liu, C. H., Thangada, S., Thopmson, B. D., and Kluk, M. (1999) *Biochem. Pharmacol. 58*, 201−207.
42. Mendez, A. J., Oram, J. F., and Biermann, E. L. (1991) *J. Biol. Chem. 266*, 10104−10111.
43. Desai, N. N., Carlson, R. O., Mattie, M. E., Olivera, A., Buckley, N. E., Seki, G., Brooker, G., and Spiegel, S. (1995) *J. Cell. Biol. 121*, 1385−1395.
44. Seufferlein, T., and Rozengurt, E. (1995) *J. Biol. Chem. 270*, 24334−24342.
45. Chin, T. Y., and Chueh, S. H. (1998) *Am. J. Physiol. 275*, C1255−C1263.
46. Desai, N. N., and Spiegel, S. (1991) *Biochem. Biophys. Res. Commun. 181*, 361−366.
47. Okajima, F., and Kondo, Y. (1995) *J. Biol. Chem. 270*, 26332−26340.
48. Chun, J., Contos, J. J., and Munroe, D. (1999) *Cell Biochem. Biophys. 30*, 231−242.

BI001162A